

Composite zinc/silicon nanocrystalline thin film: preparation, structures and the effect of oxidation on their photoluminescence

This article has been downloaded from IOPscience. Please scroll down to see the full text article.

2001 J. Phys.: Condens. Matter 13 787

(<http://iopscience.iop.org/0953-8984/13/5/301>)

View [the table of contents for this issue](#), or go to the [journal homepage](#) for more

Download details:

IP Address: 171.66.16.226

The article was downloaded on 16/05/2010 at 08:25

Please note that [terms and conditions apply](#).

Composite zinc/silicon nanocrystalline thin film: preparation, structures and the effect of oxidation on their photoluminescence

Y Zhu, H Wang and P P Ong¹

Department of Physics, National University of Singapore, 10 Kent Ridge Crescent, Singapore 119260

E-mail: phyongpp@nus.edu.sg

Received 30 August 2000

Abstract

Zinc/silicon nanocrystalline thin films were prepared by the pulsed laser deposition method in a vacuum chamber using a rotary target which exposed the zinc and silicon materials to the laser alternately. TEM, EDS, AFM, SIMS and XPS results show that the as-prepared sample was a mixture of silicon and zinc nanoparticles, which were only slightly oxidized. The existence of silicon nanocrystals was also confirmed by photoluminescence analysis. XPS results confirmed that, when the samples were annealed in the open but clean atmosphere, the extent of oxidation of the film increased with temperature. When the temperature was increased from room temperature to 500 °C, the intensity of the photoluminescence peak from the nanosilicon crystals first increased, then decreased and finally disappeared. A new PL peak found in the wavelength region of 400–550 nm was attributed to ZnO nanoparticles formed by their interaction with silicon oxide. Our results confirmed that the interface effect between the Si and Zn nanoparticles strongly affects the PL of the interfacial ZnO nanoparticles.

1. Introduction

In recent years, low dimensional semiconductor composites have attracted much interest due to their special photoluminescence (PL) properties [1, 2], especially visible PL at room temperature of nanometre-sized silicon materials [3–7]. Much study was focused on silicon-based or other light-emitting materials, modification of their optical properties [8] and their probable applications in devices such as electronics, optoelectronics and sensors [9, 10]. Studies of ZnO particles have been carried out extensively as it is a well known semiconductor that exhibits an efficient blue–green emission and is a promising material for electroluminescent devices such as vacuum fluorescent and field-emission displays, especially flat panel

¹ Corresponding author.

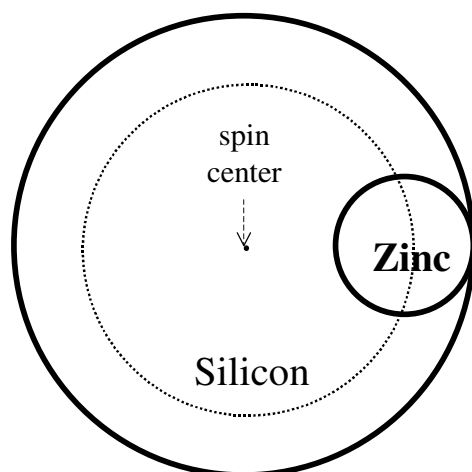


Figure 1. Schematic diagram of zinc/silicon rotary target assembly for laser ablation in PLD.

displays [11], and laser applications [12]. In a nanoparticle, unlike in bulk material, the influence of the surface cannot be ignored. Indeed, it is well known that surface defects play an important role in the luminescence processes. However, luminescent properties of the surface exciton in ZnO are still not well understood [13].

In this paper we report the fabrication of composite zinc/silicon nanocrystalline thin films and their structures and properties. PL of the silicon nanoparticles appeared in the original sample and those annealed at low temperatures, whereas PL of the ZnO nanoparticles appeared in the high-temperature-annealed samples. This result confirmed that the PL of the ZnO nanoparticles is very much affected by the nature of the surface interaction between the Si and ZnO nanoparticles. It follows from this observation that it should be possible to modify the PL property of the ZnO nanoparticles by controlling its surrounding materials.

2. Experiment

The zinc/silicon thin films were deposited on a substrate by the pulsed laser deposition (PLD) method. A Nd:YAG pulsed laser beam (Spectra-Physics, GCR-170) of 355 nm wavelength was used to ablate a two-material rotary target (see figure 1) in an ultrahigh vacuum chamber. The ablation target was first prepared from one piece of high purity (99.99%) zinc plate (12.5 mm in diameter) and one 99.999% Si round plate wafer of diameter $D = 50$ mm. The Zn plate was glued onto the surface of the silicon wafer, creating an assembly of the two composite materials, which were in physical, but not chemical, contact. During the PLD process, the centre of the zinc–silicon target was set to spin about its central axis so that the silicon and zinc materials were alternately ablated, evaporated and finally deposited onto the substrate. All the glass and Si wafer substrates were first thoroughly cleaned in an acetone ultrasonic bath and dried up. The growth of the thin films was carried out in a high vacuum system with a background pressure of about 8×10^{-8} mbar. The laser deposition was carried out for 40 minutes, with the target rotating at about 1.2 rounds/minute. From the ablated circles marked on the target surface, the ratio of the exposed areas of Si and Zn under the laser ablation was calculated to be about 1:6 in our present experiments.

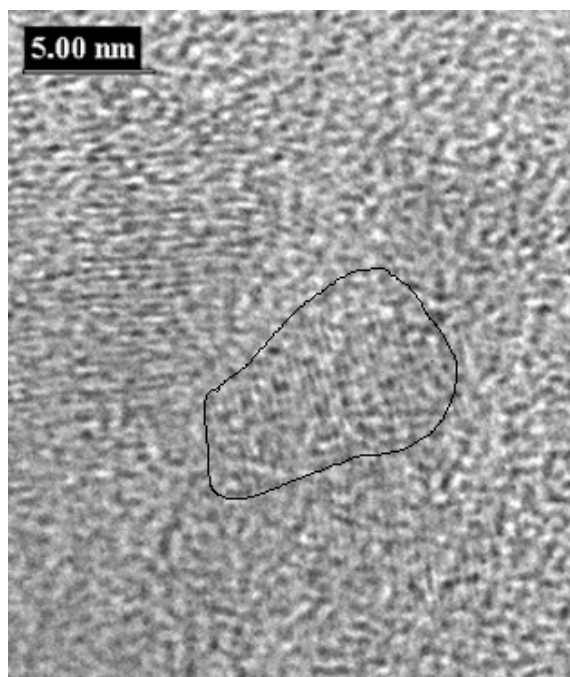


Figure 2. TEM photograph of the as-prepared film showing typical nanocrystals.

For the x-ray photoelectron spectroscopy (XPS) and photoluminescence (PL) studies, the samples investigated were the as-prepared sample, and those annealed at 300, 400 and 500 °C for 1 hour, and at 500 °C for 6 hours. These samples will be respectively referred to as samples (a)–(e). All annealing was done in the open but clean atmosphere. XPS measurements were carried out on a VG ESCALAB mark II spectrometer. A Mg K α source (1253.6 eV photons) was used with the analyser mode set at a constant analyser energy of 20 eV. The x-ray source was run at 150 W (15 kV and 10 mA). The PL measurements were carried out with a fluorescence spectrophotometer (Perkin Elmer, LS 50B) using an excitation light wavelength of 280 nm. The light source used was a 300 W Xe lamp. Atomic force microscopy (AFM) (DI 3000 SPM with IIIa controller) and secondary ion mass spectroscopy (SIMS) were used to analyse the structures of the samples. SIMS measurements were carried out using the CAMECA IMS 6F instrument with a Cs⁺ ion beam, and with the vacuum at about 6×10^{-10} Torr, the ion current at 15 nA and the ion energy at 5 keV.

3. Results and discussion

Figure 2 is a transmission electron microscope (TEM) photograph of the film showing the presence of crystalline nanoparticles. A typical nanocrystal is shown in the contoured curve on the photograph. The particles were typically about 15 nm in diameter. Figure 3 depicts the energy dispersive x-ray spectroscopy (EDS) results on the composition of the as-prepared film. Cu and C are present in both spectra because the sample holder consisted of a carbon film resting on a copper grid. On the site of one kind of crystalline nanoparticle (upper curve) the respective Zn and silicon peak intensities are high while that of oxygen is fairly low. On the site of another kind of crystalline nanoparticle (lower curve) the oxygen and Zn peak intensities

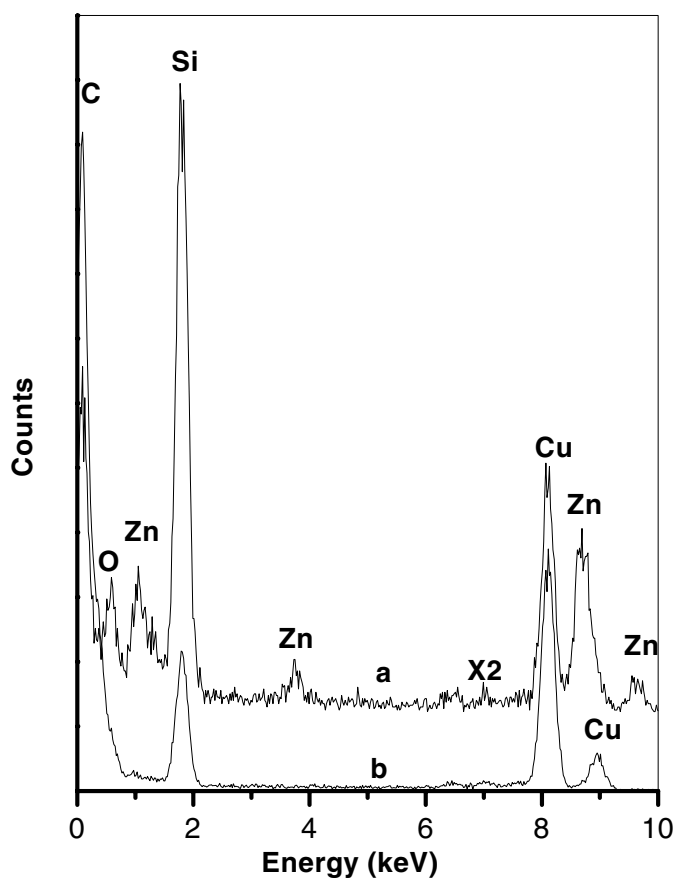


Figure 3. EDS results on the composition of the film. Upper curve: on the site of one kind of crystalline nanoparticle, Zn and silicon peak intensities are high while the oxygen peak intensity is low. Lower curve: on the site of another kind of crystalline nanoparticle, the oxygen and Zn peak intensities almost disappear while the silicon peak intensity remains high. '×2' on the upper curve indicates that its vertical scaling has been doubled.

almost disappear while that of silicon remains high. These spectra indicate that there are two types of nanoparticle whose material compositions are either pure silicon or silicon mixed with Zn. The low oxygen peak intensity in either case provides evidence that the nanoparticle surface layers for the as-prepared film are only slightly oxidized. In figure 4, the AFM image of the as-prepared sample shows that the film was composed of nanoparticles of about 20 nm in diameter but with a few of them larger than 50 nm. This result is somewhat different from the TEM results as TEM shows the actual crystal size while the AFM image is obtained from the change in particle boundary. Figure 5 gives the SIMS depth profiles of the same film for Si, Zn and O. It also indicates that the film thickness was about 250 nm. The smooth variation of the Si and Zn profiles indicates that the structure was a fairly homogeneous mixture of zinc and silicon. The oxygen content in the film was generally low, and became still lower with increasing depth, indicating that the as-prepared film was only slightly oxidized, mostly at or near the film surface.

Figure 6 shows the XPS results for the Zn 2p peaks for all the five samples measured. Curve (a) represents the results for the as-prepared sample, and curves (b)–(e) are for the

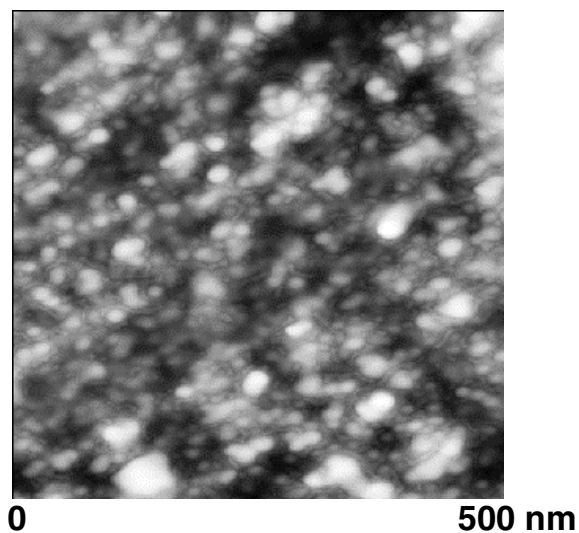


Figure 4. AFM image of the as-prepared zinc/silicon film.

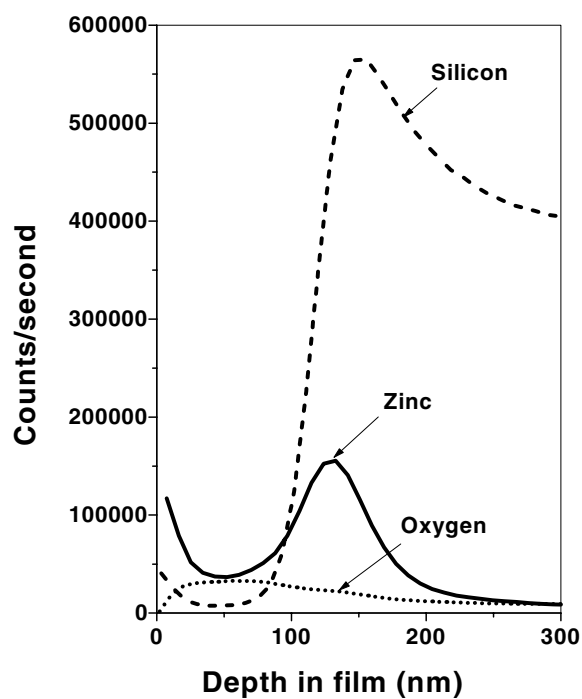


Figure 5. SIMS depth profiles of the as-prepared sample for Si, Zn and O.

corresponding annealed samples. A small energy scale correction on the x -axis against electrostatic charge effect was applied to all the results. In order to avoid overlapping of the curves, they were arbitrarily displaced vertically with respect to one another. It can be seen from the results that the peak positions, shapes and sizes change gradually with increasing

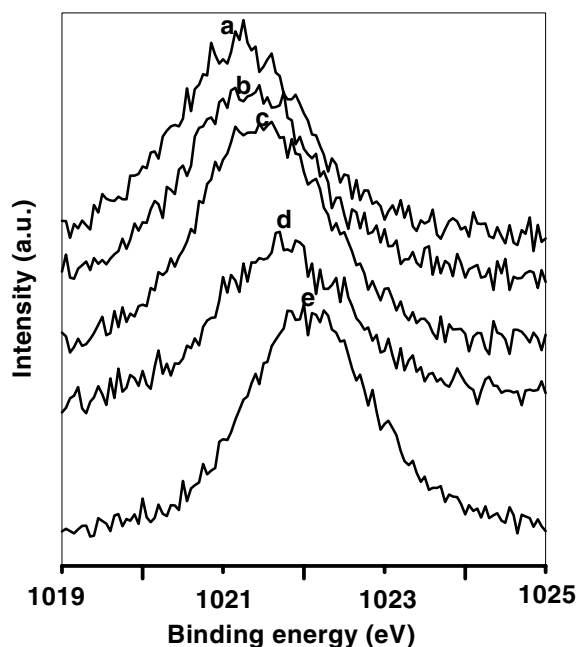


Figure 6. XPS results for the Zn 2p peaks for all the five samples: (a) as-prepared sample; (b) sample annealed at 300 °C for 1 hour; (c) sample annealed at 400 °C for 1 hour; (d) sample annealed at 500 °C for 1 hour and (e) sample annealed at 500 °C for 6 hours.

annealing time and temperature. As the samples were annealed in the open atmosphere, this change of the XPS spectrum was most likely due to the gradual oxidation of zinc. It is consistent with the observed gradual shift towards higher binding energy of the Zn 2p peak, since the bonding energy of the oxidized zinc element is higher than that of pure zinc. Therefore, our results suggest that the extent of oxidation of Zn increased gradually with the sample annealing temperature until, at saturation, all the zinc bonds were finally terminated with O when the sample was annealed at 500 °C for 6 hours.

Figure 7 shows the PL results for all the samples in the wavelength region of 300–550 nm. The silicon PL peak of sample (a) is almost the same as that of the silicon nanocrystals prepared by direct dc sputtering of the silicon material onto the liquid nitrogen-cooled surface of the stainless steel trap [14]. For sample (b), which was annealed at 300 °C for 1 hour, the silicon PL peak intensity was much higher than that of sample (a). For sample (c), which was annealed at 400 °C for 1 hour, this peak intensity dropped drastically. Instead two new peaks appeared; one was a very sharp peak at about 400 nm, while the other was a broad peak at about 440 nm. For sample (d), which was annealed at 500 °C for 1 hour, both the silicon PL peak and the sharp PL peak disappeared completely, while the PL peak at 440 nm increased slightly. With further annealing at 500 °C for 6 hours (curve (e)), there was little further change in the peak at 440 nm, as compared with that of sample (d).

Since the PL peak of the original sample (a) was almost the same as that of sample (f) obtained from the pure silicon nanoparticles (prepared by direct dc sputtering of the silicon material onto the liquid-nitrogen-cooled surface of the stainless steel trap), we can infer that the PL emission in sample (a) also originated from the silicon nanoparticles of the film. When the sample was annealed at 300 °C (sample (b)), the tiny silicon clusters gathered

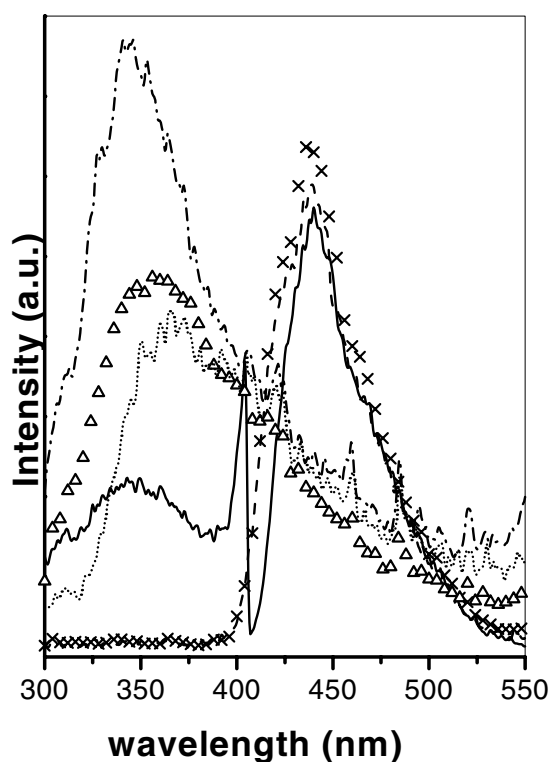


Figure 7. PL results for all the samples (a)–(e) as defined in figure 4. Curve (a) is drawn with open triangles; (b) with a dot–dash line; (c) with a continuous line; (d) with a dashed line; and (e) with crosses. Also included for comparison is curve (f) as a dotted line for the PL of a sample of a pure Si nanocrystal film produced by the direct dc sputtering method [14].

together and aggregated into silicon nanoparticles, thereby producing a large increase in the PL emission. It has been reported that quantum confinement of carriers in nanocrystalline Si enlarges the band gap of nanometre-sized Si structures giving rise to the room temperature PL [15]. When the sample was more intensely annealed at 400 °C (sample (c)), some of the silicon nanoparticles aggregated so much that they became coarse particles. In consequence, no quantum confinement effect appeared for the coarse particles, resulting in a corresponding decrease in PL emission from them. This change in quantum confinement effect is also evident from the shift in the PL Si peaks, but not in the Zn (ZnO) peaks, with different annealing conditions. Therefore, the origin of the high-intensity luminescence is probably a consequence of quantum confinement in the silicon nanoparticles [3, 14, 15]. At still higher annealing temperatures (samples (d) and (e)), most of the remaining silicon nanoparticles were either completely oxidized or aggregated into very large particles, so that the silicon PL peak disappeared altogether. Of the two new peaks appearing at the high annealing temperature of 400 °C, the very sharp one at 400 nm, which had little or no size distribution effect, might come from some transient interface of the silicon–zinc, as it only appeared in a very narrow range of annealing temperatures and wavelengths. The PL peak at about 440 nm was possibly attributed to the formation of ZnO nanoparticles and their interactions with silicon oxide. This is consistent with the interpretation of the change in the XPS Zn 2p peak seen in figure 6 when the annealing temperature was increased to 400 °C. It suggests that some of the zinc particles

were oxidized even when they were inside the film and surrounded by silicon or oxidized silicon. For sample (d) annealed at 500 °C for 1 hour, more zinc particles were oxidized until finally, for the sample annealed at 500 °C for 6 hours, all the zinc particles were completely oxidized. The eventual saturation in oxidation of Zn to ZnO explains why there was a small further shift of the PL peak position in the transition from sample (d) to (e).

The position of our ZnO PL peak is different from that of van Dijken *et al* [16] in which the nanocrystalline ZnO was suspended in 2-propanol. They obtained a strong and broad visible PL spectrum with its maximum lying between 500 and 530 nm. Although our PL peak wavelength region is within theirs, our PL peak is narrower, and its position is at a shorter wavelength. This large difference arises because their ZnO particles were in a quasi-free surface (suspension) whereas ours were confined by silicon or oxidized silicon. This suggests that the PL emission is strongly enhanced by surface states of the ZnO nanoparticles. Thus, in principle, it should be possible to modify the PL emission properties by modifying the surface states of the ZnO particles.

4. Conclusion

Zinc/silicon nanocrystalline thin films were successfully prepared by the pulsed laser deposition method in the vacuum condition by using a two-material rotary target to alternately ablate the silicon and zinc materials and deposit them onto a substrate. The as-prepared sample was found to be a homogeneous mixture of silicon and zinc nanoparticles, both of which were only slightly oxidized. When the film was annealed in the open but clean atmosphere, the extent of oxidation increased with intensity of annealing. With increasing annealing, the PL peak intensity from the nanosilicon crystals first increased, then decreased, and finally disappeared. A new PL peak which appeared in the wavelength region of 400–550 nm when the sample was annealed at 400 °C or higher was attributed to the formation of ZnO nanoparticles and their interaction with silicon oxide. The surface states in the interface region between the ZnO particles and their surrounding have a very important effect on the emission properties of ZnO.

Acknowledgments

We would like to thank Dr Q T Li for the use of the PL apparatus, Dr Wee Thye Shen Andrew for the use of the SIMS instrument, and Ms B K Tan, Messrs H H Teo, H K Wong and Y Liu for their experimental assistance. This work was supported under NUS research grant no R-144-000-011-112.

References

- [1] Hayashi S and Yamamoto K 1996 *J. Luminesc.* **70** 352
- [2] Meada Y, Tsukamoto N, Yazawa Y, Kamemitsu Y and Masumoto Y 1991 *Appl. Phys. Lett.* **59** 3168
- [3] Caham L T 1990 *Appl. Phys. Lett.* **57** 1046
- [4] Wilcoxon J P and Samara G A 1999 *Appl. Phys. Lett.* **74** 3164
- [5] Takagi H, Ogawa H, Yamazaki Y, Ishizaki A and Nakagiri T 1990 *Appl. Phys. Lett.* **56** 2379
- [6] Shimizu-Iwayama T, Nakao S and Saitoh K 1994 *Appl. Phys. Lett.* **65** 1841
- [7] Littau K A, Szajowski P J, Muller A J and Brus L E 1993 *J. Phys. Chem.* **97** 1224
- [8] Ohtsuka S, Koyama K and Tanaka S 1994 *Int. Symp. on Nonlinear Photonic Matter (Tokyo, 1994)* extended abstract, p 207
- [9] Roxlo C B, Deckman H W and Abeles B 1986 *Phys. Rev. Lett.* **A 57** 2462
- [10] Morales A M and Lieber C M 1998 *Science* **279** 208
- [11] Shionoya S and Yen W M (eds) 1999 *Phosphor Handbook* (Boca Raton, FL: Chemical Rubber Company)

- [12] Cao H, Zhao Y G, Ho S T, Seelig E W, Wang Q H and Chang R P H 1999 *Phys. Rev. Lett.* **82** 2278
- [13] Harada Y, Kondo N, Ichimura N and Hashimoto S 2000 *J. Luminesc.* **87–89** 405
- [14] Zhu Y, Wang H and Ong P P 2000 *J. Phys. D: Appl. Phys.* **33** 1965
- [15] Cullis A G, Canham L T and Calcott P D J 1997 *J. Appl. Phys.* **82** 909
- [16] van Dijken A, Meulenkaamp E A, Vanmaekelbergh D and Meijerink A 2000 *J. Luminesc.* **87–89** 454